PHOTOACOUSTIC IMAGE RECONSTRUCTION FROM A FREQUENCY-INVARIANT SOURCE LOCALIZATION PERSPECTIVE

S. M. Akramus Salehin, and T. D. Abhayapala

College of Engineering and Computer Science, Australian National University
Canberra, ACT 0200, Australia
email: asalehin@rsise.anu.edu.au, thushara.abhayapala@anu.edu.au

ABSTRACT

Photoacoustic imaging provides high spatial resolution images of biological tissues and is useful for molecular imaging. The exact reconstruction algorithms for photoacoustic imaging are either slow or assume a continuous sensor with infinite bandwidth. We propose a novel reconstruction method which expands the source distribution function in the Fourier-Bessel domain. The source distribution can be reconstructed from frequency samples corresponding to the Bessel zeros. Sparsity of the source distribution in the Fourier-Bessel domain makes reconstruction faster. Further, this method was extended to the discrete aperture and a condition was derived to avoid spatial aliasing. The proposed method was verified using numerical simulations.

1. INTRODUCTION

Photoacoustic imaging is done by measuring the acoustic waves generated by soft tissue due to the absorption of electromagnetic (EM) energy from optical or radio waves. Ultrasound sensors placed on the surface of these tissues record these acoustic waves from which the distribution of the EM absorption can be computed. This electromagnetic absorption is a property related to the type of tissue. Moreover, photoacoustic imaging can provide a very high spatial resolution and is used for cancer detection, breast imaging, small animal imaging and molecular imaging.

We address the problem of estimating the absorption distribution from the measured data. Approximate reconstruction algorithms include the statistical approach [9] and delay and sum beamforming [2]. Exact solutions both in the time and frequency domain were provided in [7, 8], but they considered a continuous aperture and infinite bandwidth.

In this paper we propose a novel method that expands the source distribution function in the Fourier-Bessel domain. To reconstruct the source distribution, we estimate the Fourier-Bessel coefficients from frequency samples corresponding to the Bessel zeros. The proposed method does not require infinite bandwidth and conditions for exact reconstruction for the finite bandwidth case is provided. Further, this method was extended for discrete apertures and a rule was derived to avoid spatial aliasing. The proposed method is faster than Fourier-Domain methods since it only uses a subset of frequency samples and can exploit sparsity of the source distribution in the Fourier-Bessel domain.

This paper is arranged as follows: Section 2 provides background to photoacoustic imaging, Section 3 describes the modal expansion of the 2D Green's functions and Section 4 introduces the Fourier-Bessel expansion of the source distribution. We compare our proposed algorithm to previous Fourier-Domain methods and extend it for discrete apertures with spatial filtering in Section 5. Section 6 provides an extension to spherical geometries and Section 7 describes numerical experiments conducted and the results obtained to validate our method. Section 8 summarizes the main ideas of this paper.

Notation: bold lowercase letters represents vectors.

2. PHOTOACOUSTIC THEORY

In this section we provide a short review of the wave equations for photoacoustic, the reader is referred to [4] which provides an extensive review of photoacoustic theory.

Provided that thermal diffusion and kinetic viscosity is ignored, the inhomogeneous Helmholtz equation relating the heating function $H(\boldsymbol{x},t)$ and the pressure $p(\boldsymbol{x},t)$ at a vector position $\boldsymbol{x}$ and time t is

$$\nabla^2 p(\boldsymbol{x},t) - \frac{1}{c^2}\frac{\partial}{\partial t^2}p(\boldsymbol{x},t) = -\frac{\rho}{C_p}\frac{\partial}{\partial t}H(\boldsymbol{x},t). \qquad (1)$$

Here c denotes the speed of sound which is assumed to be constant, C_p is the specific heat capacity, ρ is the isobaric volume expansion coefficient and the heating function $H(\boldsymbol{x},t)$ is defined as the thermal energy deposited per unit time and volume. Further, the heating function is a product of the source distribution function $A(\boldsymbol{x})$ (commonly referred to as spatial absorption function in literature [7, 8]) and the temporal illumination function $I(t)$

$$H(\boldsymbol{x},t) = A(\boldsymbol{x})I(t). \qquad (2)$$

Assuming the photo illumination or the RF pulse duration is short, the temporal illumination function can be approximated as a Dirac delta function, $I(t) = \delta(t)$. Therefore, the solution to the inhomogeneous Helmholtz equation (1) based on the Green's function can be expressed as

$$p(\boldsymbol{x}_s,t) = \eta \iiint_S A(\boldsymbol{x})\frac{\delta'(t-\frac{||\boldsymbol{x}_s-\boldsymbol{x}||}{c})}{4\pi||\boldsymbol{x}_s-\boldsymbol{x}||}\,\mathrm{d}S \qquad (3)$$

where $\eta = \rho/C_p$, $\delta'(t) = \partial\delta(t)/\partial t$, S is the volume of region under test and $\boldsymbol{x}_s$ is the vector position of the ultrasound sensors. The pressure $p(\boldsymbol{x}_s,t)$ also represents the time domain signal received by a ultrasound sensor placed at $\boldsymbol{x}_s$. The Fourier transform of (3) yields

$$p(\boldsymbol{x}_s,k) = -ikc\eta \iiint_S A(\boldsymbol{x})G(k;\boldsymbol{x}_s,\boldsymbol{x})\,\mathrm{d}S \qquad (4)$$

S.M.A. Salehin is also associated with National ICT Australia, Canberra, Australia. National ICT Australia is funded through the Australian Governments Backing Australias Ability initiative and in part through the Australian Research Council.

 ISSN 2076-1465

where wavenumber $k = 2\pi f/c$ with f as the frequency of sound and $G(k;\boldsymbol{x}_s,\boldsymbol{x})$ is the Green's function. Moreover, the Fourier transform analysis and synthesis equations applied to the recorded signals are defined respectively as

$$p(\boldsymbol{x}_s,k) = \int_{-\infty}^{+\infty} p(\boldsymbol{x}_s,t)e^{i(k/c)t}\,\mathrm{d}t \tag{5}$$

and

$$p(\boldsymbol{x}_s,t) = \frac{1}{2\pi}\int_{-\infty}^{+\infty} p(\boldsymbol{x}_s,k)e^{-i(k/c)t}\,\mathrm{d}k. \tag{6}$$

The estimation of the source distribution function $A(\boldsymbol{x})$ from measurements at several positions outside the source region is an inverse problem. By analyzing (4), we can deduce that the source distribution function is frequency invariant, i.e. the source distribution function is the same for all frequencies. Hence, in this paper, the problem of estimating $A(\boldsymbol{x})$ is labeled as a frequency invariant source localization problem.

3. 2D GREEN'S FUNCTION

The Green's function in 2D for the exterior case where all the sources are enclosed by the sensors is

$$G(k;\boldsymbol{x}_s,\boldsymbol{x}) = \frac{i}{4}H_0^{(1)}(k||\boldsymbol{x}_s-\boldsymbol{x}||) \tag{7}$$

where $H_0^{(1)}(\cdot)$ is the Hankel function of the first kind and order zero. Using polar co-ordinates, with position vectors $\boldsymbol{x}_s$ and $\boldsymbol{x}$ with radial position of x_s and x; and angular positions ϕ_s and ϕ respectively, then the addition theorem can be used to expand the 2D Green's function [6] as

$$H_0^{(1)}(k||\boldsymbol{x}_s-\boldsymbol{x}||) = \sum_{n=-\infty}^{\infty} H_n^{(1)}(kx_s)J_n(kx)e^{-in\phi}e^{in\phi_s} \tag{8}$$

which is valid when $x_s > x$ and $J_n(\cdot)$ represents a Bessel function of order n. This expansion is called eigen basis or modal expansion of the Green's function and was used for ultrasound reflectivity imaging [3].

4. SOURCE DISTRIBUTION EXPANSION

We define the 2D Fourier-Bessel expansion of the source distribution function as

$$A(\boldsymbol{x}) = \sum_{m=-\infty}^{\infty}\sum_{\ell=1}^{\infty}\beta_{m\ell}J_m\left(\frac{z_\ell^m}{r_0}x\right)e^{im\phi} \tag{9}$$

where $i=\sqrt{-1}$, z_ℓ^m is the ℓ^{th} root of $J_m(\cdot)$, $\beta_{m\ell}$ are complex Fourier-Bessel coefficients where m is called the mode and ℓ is the index. The source distribution function can represented by its sample values, however by expanding the source distribution function in a different domain a more compact representation is possible requiring estimation of fewer terms in order to obtain $A(\boldsymbol{x})$. The next section describes a method to estimate $\beta_{m\ell}$ to reconstruct the source distribution.

5. ESTIMATION OF SOURCE DISTRIBUTION

Given that the ultrasound sensors are placed uniformly at a radius $R > r_0$, and assuming that $A(\boldsymbol{x})$ is zero at all radii greater than r_0 then the signal received by a sensor at angular position ϕ_s and wavenumber k for the 2D case can be specified as

$$p_R(\phi_s,k) = -ikc\eta\int_0^{r_0}\int_0^{2\pi} A(\boldsymbol{x})G(k;\boldsymbol{x}_s,\boldsymbol{x})\,\mathrm{d}\phi\,x\mathrm{d}x. \tag{10}$$

Substituting (9) and (8) into (10) yields

$$\begin{aligned} p_R(\phi_s,k) =& \frac{kc\eta}{4}\sum_{n=-\infty}^{\infty}\sum_{m=-\infty}^{\infty}\sum_{\ell=1}^{\infty}H_n^{(1)}(kR)e^{in\phi_s} \\ &\times\int_0^{r_0}\beta_{m\ell}J_m\left(\frac{z_\ell^m}{r_0}x\right)J_n(kx)\,x\mathrm{d}x \\ &\times\int_0^{2\pi}e^{im\phi}e^{-in\phi}\,\mathrm{d}\phi. \end{aligned} \tag{11}$$

Further, we use the orthogonality property of exponential functions

$$\int_0^{2\pi}e^{im\phi}e^{-in\phi}\,\mathrm{d}\phi = \begin{cases}2\pi & \text{if } n=m,\\ 0 & \text{otherwise.}\end{cases} \tag{12}$$

to simplify (11) to

$$p_R(\phi_s,k) = \sum_{m=-\infty}^{\infty} a_m(k)e^{im\phi_s} \tag{13}$$

where

$$\begin{aligned} a_m(k) =& \frac{\pi kc\eta}{2}H_m^{(1)}(kR)\sum_{\ell=1}^{\infty}\beta_{m\ell} \\ &\times\int_0^{r_0}J_m(kx)J_m\left(\frac{z_\ell^m}{r_0}x\right)x\mathrm{d}x. \end{aligned} \tag{14}$$

Note that (13) is the spatial Fourier series expansion of the received signal on a continuous aperture as a function of the aperture angle ϕ.

We can estimate the $a_m(k)$ from the sensor recordings $p_R(\phi_s,k)$ by using the Fourier series analysis equation

$$a_m(k) = \frac{1}{2\pi}\int_0^{2\pi}p_R(\phi_s,k)e^{-im\phi_s}\,\mathrm{d}\phi_s. \tag{15}$$

We refer to $a_m(k)$ as modal coefficients and these outline the angular distribution of the source function.

5.1 Frequency-Radial Duality

The following theorem shows how to estimate the source distribution coefficients $\beta_{m\ell}$ using modal coefficients at a specific set of frequencies.

Theorem 5.1 (Frequency-Radial duality)**.** *For each mode, taking measurements at frequencies $k = z_\ell^{(m)}/r_0$ for the different zero indices ℓ we can obtain the 2D Fourier-Bessel coefficients, which expands the angular modal basis expansion to incorporate radial variations. We calculate $\beta_{m\ell}$ by*

$$\beta_{m\ell} = h_{m\ell}a_m\left(\frac{z_\ell^m}{r_0}\right) \tag{16}$$

where

$$h_{m\ell} = \frac{4}{\pi kc\eta r_0^2 H_m^{(1)}\left(\frac{z_\ell^m}{r_0}R\right)[J_{m+1}(z_\ell^m)]^2} \tag{17}$$

Proof. We use the orthogonality relationship for Bessel functions [1],

$$\int_0^{r_0} J_m\left(\frac{z_{\ell'}^m}{r_0}x\right) J_m\left(\frac{z_\ell^m}{r_0}x\right) x\mathrm{d}x = \begin{cases} \frac{r_0^2}{2}[J_{m+1}(z_\ell^m)]^2 & \text{if } \ell = \ell', \\ 0 & \text{otherwise.} \end{cases} \tag{18}$$

in (14) at $k = z_\ell^m / r_0$ to obtain

$$a_m\left(\frac{z_\ell^m}{r_0}\right) = \frac{\pi k c \eta}{2} H_m^{(1)}(kR)\beta_{m\ell}\frac{r_0^2}{2}[J_{m+1}(z_\ell^m)]^2 \tag{19}$$

By applying the definition of $h_{m\ell}$ provided by (17) in (19) we obtain (16). □

5.2 Comparison with Fourier Domain Methods

This section begins with a brief overview of the Fourier Domain algorithms, first proposed for ultrasound imaging [3] and then modified for photoacoustic imaging [7, 8]. This algorithm described in 2D expands the source distribution function as

$$A(\boldsymbol{x}) = \sum_{m=0}^{\infty} \int_0^{\infty} \alpha_m(k) k J_m(kx)\, \mathrm{d}k\, e^{im\phi} \tag{20}$$

and expands the measured signals as

$$p(\boldsymbol{x}_s, k) = \sum_{m=0}^{\infty} \hat{\alpha}_m(k) e^{im\phi_s}. \tag{21}$$

We can calculate $\hat{\alpha}_m(k)$ by the inverse of (21) (a transform similar to (15)) over all the sensors which are placed in a circle. From $\hat{\alpha}_m(k)$, we get $\alpha_m(k)$ by

$$\alpha_m(k) = \frac{\hat{\alpha}_m(k)}{c(k)H_m^{(1)}(kR)} \tag{22}$$

where $c(k)$ is a constant equal to $\pi k c \eta/2$. To compute $A(\boldsymbol{x})$ at a particular point, we take the Hankel transform over k of $\alpha_m(k)$ and then sum over the modes (20). Note that $\alpha_m(k)$ is equivalent to $\int_0^R \int_0^{2\pi} A(\boldsymbol{x}) J_m(kx) e^{-im\phi} x\, \mathrm{d}x\, \mathrm{d}\phi$ and the orthogonality of the bessel functions over an infinite interval [1]

$$\int_0^{\infty} k J_m(kx) J_m(kx')\, \mathrm{d}k = \frac{1}{x}\delta(x - x') \tag{23}$$

is used to recover the source distribution at a particular vector position $\boldsymbol{x}$, shown in (20). One of the drawbacks of the Fourier-Domain methods are that they are computationally expensive requiring the sum of a large number of terms at every point, see (20). Further, Fourier-Domain methods require an infinite bandwidth otherwise the relationship shown in (23) is no longer valid. The Fourier-Domain method was modified in [7,8] to recover the source distribution in the time domain reducing the computational complexity.

Rather than integrating over a frequency range, the proposed algorithm considers the natural integration that occurs as a wave propagates through a region of space and is therefore not affected by the spatial sampling issues due to a discrete sensor. The concept of frequency-radial duality introduced in this paper is novel and has not been utilized previously for photoacoustic imaging or ultrasound imaging. Further, given that we know that the source distribution is bounded in a radial region r_0, we need to only consider frequencies corresponding to the bessel zeros $f = cz_l^m/(2\pi r_0)$ and these frequencies are only resolved to a single mode. In addition, the source distribution can be sparse in the Fourier-Bessel domain and summation can be done over only the largest modes and indices. These lead to a large reduction in computational complexity compared to the Fourier-Domain methods where all frequencies are used and resolved to all modes. It is important to mention that a lower bound r_0 only means that less frequency samples are used and has no effect on the resolution of the reconstructed image.

One pertinent question in photoacoustic imaging is how to recover the image with a discrete aperture and avoid distortions due to spatial aliasing. Both the Fourier-domain and the time-domain methods require infinite bandwidth and a continuous aperture. Theoretical validation to their extension to the discrete and finite bandwidth case has not been provided. The next two sections highlight the advantages of our approach in considering a discrete aperture and spatial aliasing.

5.3 Discrete Aperture

In the previous sections, estimation of the Fourier-Bessel coefficients were done assuming ideal conditions with infinite bandwidth and a continuous aperture. Exact reconstruction of the source distribution $A(\boldsymbol{x})$ is possible under these ideal conditions since the source Fourier-Bessel expansion consists of a sum of infinitely many orthogonal functions. In this section we provide the conditions under which the source distribution can be reconstructed with a discrete aperture and a bandwidth limited by the frequency response of the ultrasound transducer.

Provided there are Q uniformly placed sensors at a radius R, then the discrete aperture response at a wavenumber k, as a vector is

$$\hat{\boldsymbol{p}}_R(\phi_s, k) = [p_R(\phi_s^{(1)}, k),\ \ldots,\ p_R(\phi_s^{(Q)}, k)]^T \tag{24}$$

where $\phi_s^{(q)}$ is the angular position of the q^{th} sensor. The modal coefficients can be calculated as a discrete approximation to (15)

$$a_m(k) = \frac{1}{2\pi}\boldsymbol{e}(m)^T \hat{\boldsymbol{p}}_R(\phi_s, k)\, \Delta\phi_s \tag{25}$$

where

$$\boldsymbol{e}(m) = [e^{-im\phi_s^{(1)}},\ \ldots,\ e^{-im\phi_s^{(Q)}}]^T. \tag{26}$$

For the discrete aperture, both temporal and spatial aliasing can occur. Temporal aliasing can be avoided by using a sampling frequency that is greater than twice the frequency response upper limit of the transducer. Given that we need to decompose the wavefield to a finite number of modes $m \in [-M, \ldots, M]$, a minimum number of sensors are required which must satisfy

$$Q > 2M. \tag{27}$$

Additionally, the contributions of the modes higher than M should be negligible at this wavenumber in order to avoid spatial aliasing. The spatial aliasing that can occur due to overlapping of the higher modes is referred to as modal

aliasing, more details on this is provided in [5]. Therefore given a discrete number of sensors, to avoid modal aliasing the Fourier-Bessel expansion of the source distribution should be bandlimited, i.e. coefficients for modes greater than M should be negligible for the transducer frequency response. Further, exact reconstruction of the source distribution is only possible if this expansion has significant terms for modes $m \in [-M,\ldots,M]$ and indices satisfying $k_l < z_\ell^m/r_0 < k_u$ where k_l and k_u are the lower and upper limit of the transducer frequency response respectively.

5.4 Spatial Filtering

It is important to avoid spatial aliasing since this can cause blurring and distortion in the reconstructed image. The bandlimit restriction of the source distribution to avoid aliasing limits the use of this method to practical scenario. In literature, there is currently no method prescribed to perform spatial filtering for photoacoustic image reconstruction. However, for the method described in this paper spatial filtering is possible.

The orthogonality relationship for the Bessel functions (18) can be evaluated for a continuous range of frequencies as

$$\begin{aligned}&\int_0^{r_0} J_m(kx) J_m\left(\frac{z_\ell^m}{r_0}x\right) x\mathrm{d}x \\ &= \begin{cases} \frac{r_0^2}{2}[J_{m+1}(z_\ell^m)]^2 & \text{if } k = \frac{z_\ell^m}{r_0}, \\ \frac{z_\ell^m J_{m-1}(z_\ell^m)}{k^2-(z_\ell^m/r_0)^2} J_m(kr_0) & \text{otherwise.} \end{cases}\end{aligned} \tag{28}$$

The Bessel function $J_m(kr_0)$ in (28) higher than the zeroth mode are close to zero for values of kr_0 lower than a particular upper limit. This upper limit increases with the mode number m. Using this property, a rule of thumb used in array signal processing and in source localization [5] to avoid spatial aliasing is stated as follows: the maximum number of modes present for a particular frequency response upper limit is

$$\text{minimize } m \text{ such that } m > k_u r_0. \tag{29}$$

By limiting the frequency upper limit, spatial filtering is achieved i.e. the number of modes is limited. This criterion also governs the number of sensors needed to avoid spatial aliasing with respect to frequency upper limit. Since if the number of modes is M, we require more than $2M$ sensors.

6. EXTENSION TO 3D (SPHERICAL GEOMETRY)

In this paper we have considered a 2D spatial region so that the notation is simplified and that the main ideas can be concisely described. The algorithm presented can be extended to a more practical 3D geometry where the source region is constrained within a spherical region enclosed by the sensors. Firstly the Green,s function satisfying the inhomogeneous Helmholtz equation (1) and its modal decomposition is

$$\begin{aligned}G(k;\boldsymbol{x}_s,\boldsymbol{x}) &= \frac{e^{ik\|\boldsymbol{x}_s-\boldsymbol{x}\|}}{4\pi\,\|\,\boldsymbol{x}_s-\boldsymbol{x}\,\|} \\ &= ik\sum_{n=0}^{\infty}\sum_{m=-n}^{n} h_n^{(1)}(kx_s)\, j_n(kx) Y_{mn}(\hat{\boldsymbol{x}}_s) Y_{mn}(\hat{\boldsymbol{x}})^*.\end{aligned} \tag{30}$$

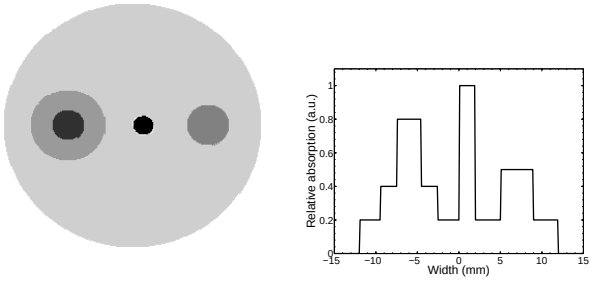

(a) (b)

Figure 1: Input sample (a) x-y view (b) x-z view through the central axis, with arbitrary units (a.u.) for the relative absorption.

where where $(\cdot)^*$ denotes the complex conjugate operator, $\hat{\boldsymbol{x}}$ and $\hat{\boldsymbol{x}}_s$ contains the azimuthal and elevation angles of the source and sensor respectively, $j_n(\cdot)$ is the spherical Bessel function, $h_n^{(1)}(\cdot)$ is the spherical Hankel function and $Y_{mn}(\cdot)$ is the spherical Harmonic function. Further the 3D Fourier-Bessel expansion of the source distribution is now as follows

$$A(\boldsymbol{x}) = \sum_{n'=0}^{\infty}\sum_{m'=-n'}^{n'}\sum_{\ell=1}^{\infty} \alpha_{n'm'}^{\ell}\, j_{n'}\left(\frac{z_\ell^{n'}}{r_0}x\right) Y_{m'n'}(\hat{\boldsymbol{x}}). \tag{31}$$

where $\alpha_{n'm'}^{\ell}$ is the 3D Fourier-Bessel coefficient with n' as the mode, m' denotes the order and ℓ denotes the index of the expansion. The procedure for 3D source reconstruction is the same as the 2D case, i.e. we calculate the coefficients of the spherical Harmonic functions at frequencies $k = z_\ell^{n'}/r_0$ to obtain $\alpha_{n'm'}^{\ell}$ which is used to reconstruct the source distribution.

7. NUMERICAL EXPERIMENTS

In this section we describe the numerical experiments performed to validate our proposed algorithm. The set up for the numerical experiment is shown in Fig. 1, with r_0 as 15mm, speed of propagation is $1.5mm/\mu s$ (speed of sound in soft tissue), the constant $\eta = 1$ and the sensors are placed in a circle at a radius of 50mm. The bandwidth of measurement is from 0 to 3MHz, this means that modes up to 180 need to be resolved (29), therefore 380 sensors are placed uniformly around the source to avoid spatial aliasing. Also, for the zeroth mode, only 60 indices can be recovered. In the numerical experiments, we approximated the signal received at the sensor for each of the required frequencies $k = z_\ell^m/r_0$ using a quadrature approximation to the double integral shown in (4).

In this work we are interested in estimating the source distribution function using snapshots differing in frequencies rather than snapshots differing in time. Therefore, the noise to be introduced in the simulations has to be defined differently. Assuming that we use frequencies in the range from k_ℓ to k_u then the power of the signal between this range is

$$P_{signal} \triangleq \frac{1}{k_u - k_\ell}\int_{k_\ell}^{k_u} |f(\omega)|^2\,\mathrm{d}\omega. \tag{32}$$

Since we are working with discrete samples, (32) is modified

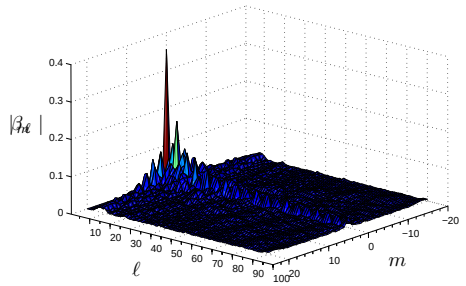

Figure 2: Magnitude of Fourier-Bessel coefficients at the modes m and indices l of the input source distribution.

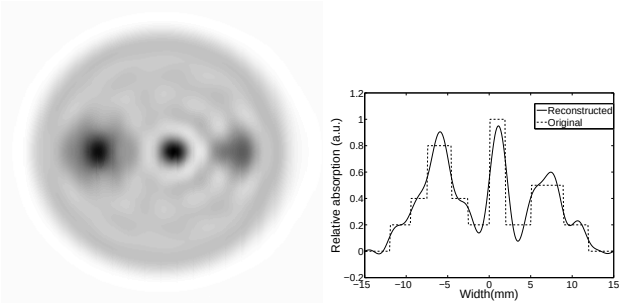

(a) (b)

Figure 3: Reconstructed image using the largest 60 estimated Fourier-Bessel coefficients at a SNR = 20dB.

to

$$P_{signal} \triangleq \frac{1}{k_u - k_\ell} \sum_{\omega=2}^{\Omega} |f(\omega)|^2 \left(\gamma(\omega) - \gamma(\omega-1)\right). \qquad (33)$$

In (33), there are Ω non-uniform, discrete samples in the frequency range of interest, $f(\omega)$ is the signal recorded at the ω^{th} frequency sample and $\gamma(\omega)$ is the frequency at sample ω, arranged in ascending order. The SNR in dB can then be defined in the normal way as $10\log_{10}(P_{signal}/\sigma_n^2)$ where σ_n^2 is the noise power. Further, the noise is AWGN. For the simulations a SNR of 20 dB was used, with 20 measurements available at each required frequency to average out the noise.

We applied our proposed method to the frequency samples in order to estimate $\beta_{m\ell}$. The values of the Fourier-Bessel coefficients of the input source distribution is shown in Fig. 2. We can observe that the magnitude of most coefficients are negligible. A reconstruction using only the largest estimated 60 Fourier-Bessel coefficients is illustrated by Fig. 3 and using 120 Fourier-Bessel coefficients is illustrated by Fig. 4. It is observed that a better reconstruction with improved resolution results if more coefficients $\beta_{m\ell}$ are used. However, this increases the computational expense.

8. SUMMARY AND CONCLUSIONS

In this paper, we have proposed a novel method for photoacoustic image reconstruction which is faster than Fourier-Domain methods and does not assume infinite bandwidth. This method can be easily discretized and a relationship between the number of sensors and upper frequency limit was provided in order to avoid spatial aliasing. In this method, we expand the source distribution in the Fourier-Bessel domain. Therefore, the source can be reconstructed by estimating the Fourier-Bessel coefficients from frequency samples corresponding to the Bessel zeros.

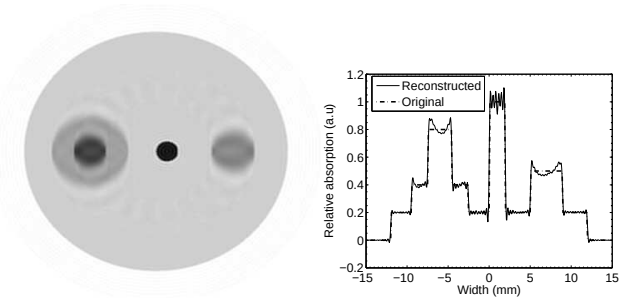

(a) (b)

Figure 4: Reconstructed image using the largest 120 estimated Fourier-Bessel coefficients at a SNR = 20dB.

REFERENCES

[1] M. Abramowitz and I. A. Stegun. *Handbook of Mathematical Functions with Formulas, Graphs, and Mathematical Tables*. New York: Wiley, 10 edition, 1972.

[2] C. G. A. Hoelen, F. F. M. de Mul, R. Pongers, and A. Dekker. Three-dimensional photoacoustic imaging of blood vessels in tissue. *Opt. Lett.*, 23(8):648–650, 1998.

[3] S. J. Norton and M. Linzer. Ultrasonic reflectivity imaging in three dimensions: Exact inverse scattering solutions for plane, cylindrical, and spherical apertures. *Biomedical Engineering, IEEE Transactions on*, BME-28(2):202–220, Feb. 1981.

[4] A. C. Tam. Applications of photoacoustic sensing techniques. *Rev. Mod. Phys.*, 58(2):381–431, Apr 1986.

[5] H. Teutsch and W. Kellermann. Acoustic source detection and localization based on wavefield decomposition using circular microphone arrays. *The Journal of the Acoustical Society of America*, 120(5):2724–2736, 2006.

[6] E. G. Williams. *Fourier Acoustics: Sound Radiation and Nearfield Acoustical Holography*. San Diego: Academic Press, 1999.

[7] M. Xu and L. Wang. Time-domain reconstruction for thermoacoustic tomography in a spherical geometry. *Medical Imaging, IEEE Transactions on*, 21(7):814–822, July 2002.

[8] M. Xu, Y. Xu, and L. Wang. Time-domain reconstruction algorithms and numerical simulations for thermoacoustic tomography in various geometries. *Biomedical Engineering, IEEE Transactions on*, 50(9):1086–1099, Sept. 2003.

[9] Y. V. Zhulina. Optimal statistical approach to optoacoustic image reconstruction. *Appl. Opt.*, 39(32):5971–5977, 2000.